nature medicine

LETTERS

https://doi.org/10.1038/s41591-019-0485-4

Meta-omics analysis of elite athletes identifies a performance-enhancing microbe that functions via lactate metabolism

Jonathan Scheiman[1,2,3,13], Jacob M. Luber[4,5,6,7,8,13], Theodore A. Chavkin[4,5,7,13], Tara MacDonald[9,10], Angela Tung[1,2], Loc-Duyen Pham[4,5], Marsha C. Wibowo[4,5,7], Renee C. Wurth[3,11], Sukanya Punthambaker[1,2], Braden T. Tierney[4,5,6,7], Zhen Yang[4,5,12], Mohammad W. Hattab[2], Julian Avila-Pacheco[8], Clary B. Clish[8], Sarah Lessard[9,10], George M. Church[1,2]* and Aleksandar D. Kostic[4,5,7]*

The human gut microbiome is linked to many states of human health and disease[1]. The metabolic repertoire of the gut microbiome is vast, but the health implications of these bacterial pathways are poorly understood. In this study, we identify a link between members of the genus *Veillonella* and exercise performance. We observed an increase in *Veillonella* relative abundance in marathon runners postmarathon and isolated a strain of *Veillonella atypica* from stool samples. Inoculation of this strain into mice significantly increased exhaustive treadmill run time. *Veillonella* utilize lactate as their sole carbon source, which prompted us to perform a shotgun metagenomic analysis in a cohort of elite athletes, finding that every gene in a major pathway metabolizing lactate to propionate is at higher relative abundance postexercise. Using $^{13}C_3$-labeled lactate in mice, we demonstrate that serum lactate crosses the epithelial barrier into the lumen of the gut. We also show that intrarectal instillation of propionate is sufficient to reproduce the increased treadmill run time performance observed with *V. atypica* gavage. Taken together, these studies reveal that *V. atypica* improves run time via its metabolic conversion of exercise-induced lactate into propionate, thereby identifying a natural, microbiome-encoded enzymatic process that enhances athletic performance.

Human microbiome studies have generally examined individuals who are 'healthy' or diseased and identified features of the microbiome associated with these states[2–4]. Athlete microbiomes have been found to contain distinct microbial compositions defined by elevated abundances of *Veillonellaceae*, *Bacteroides*, *Prevotella*, *Methanobrevibacter* or *Akkermansia*[5,6]. These studies show that exercise is associated with changes in microbiome composition, although the effects of these microbial genera on phenotype remain unknown.

To identify gut bacteria associated with athletic performance and recovery states, we recruited athletes ($n=15$) who ran in the 2015 Boston Marathon, along with a set of sedentary controls ($n=10$), and conducted 16S ribosomal DNA (rDNA) sequencing on approximately daily samples collected up to one week before and one week after marathon day ($n=209$ samples; Supplementary Tables 1 and 2). Phylum-level relative abundance partitioned by individual, time (−5 to +5 d in relation to running the marathon), and whether the participant was an athlete (Fig. 1a) showed that, at this high-level taxonomic view, any orthogonal differences were likely to be due to variation at the level of the individual. The bacterial genus *Veillonella* was the most differentially abundant microbiome feature between pre- and postexercise states (Supplementary Table 2). There was a significant difference in relative *Veillonella* abundance ($P=0.02$, Wilcoxon rank-sum test with continuity correction) between samples collected before and after exercise (Fig. 1b). To validate the significance of the association between *Veillonella* and postmarathon state, we constructed a series of generalized linear mixed-effect models (GLMMs) to predict *Veillonella* relative abundance in the marathon participants (Fig. 1c and Methods). Subsequently, significance was calculated for all of the coefficients included in the GLMM (Fig. 1d, Wald Z-tests), revealing that no coefficients were significant except time in relation to the marathon in days ($P=0.0014$, Wald Z-test; $n=15$). Both leave-one-out cross-validation (LOOCV) and iterative permutation of labels were conducted as part of the GLMM analysis (Extended Data Fig. 1 and Methods). Additionally, it appears that *Veillonella* is more prevalent among runners than non-runners (Extended Data Fig. 2), although this was not statistically significant. These correlations raise the question of whether there is a causal link between *Veillonella* and marathon runners' performance, but no conclusions can be made without proper validation.

To assess whether there are any potential benefits of *Veillonella* on performance in an animal exercise model, we designed an AB/BA crossover mouse experiment spanning 2 weeks, consisting of a control group (*Lactobacillus bulgaricus* gavage; $n=16$) and a treatment group (*Veillonella atypica* gavage; $n=16$), with a

[1]Department of Genetics, Harvard Medical School, Boston, MA, USA. [2]Wyss Institute for Biologically Inspired Engineering, Harvard University, Boston, MA, USA. [3]Fitbiomics, New York, NY, USA. [4]Section on Pathophysiology and Molecular Pharmacology, Joslin Diabetes Center, Boston, MA, USA. [5]Section on Islet Cell and Regenerative Biology, Joslin Diabetes Center, Boston, MA, USA. [6]Department of Biomedical Informatics, Harvard Medical School, Boston, MA, USA. [7]Department of Microbiology and Immunobiology, Harvard Medical School, Boston, MA, USA. [8]Broad Institute of MIT and Harvard, Cambridge, MA, USA. [9]Section on Clinical, Behavioral and Outcomes Research, Joslin Diabetes Center, Boston, MA, USA. [10]Department of Medicine, Harvard Medical School, Boston, MA, USA. [11]Department of Nutrition, Harvard T.H. Chan School of Public Health, Boston, MA, USA. [12]Department of Combinatorics and Optimization, University of Waterloo, Waterloo, Ontario, Canada. [13]These authors contributed equally: Jonathan Scheiman, Jacob M. Luber, Theodore A. Chavkin. *e-mail: gc@hms.harvard.edu; aleksandar.kostic@joslin.harvard.edu

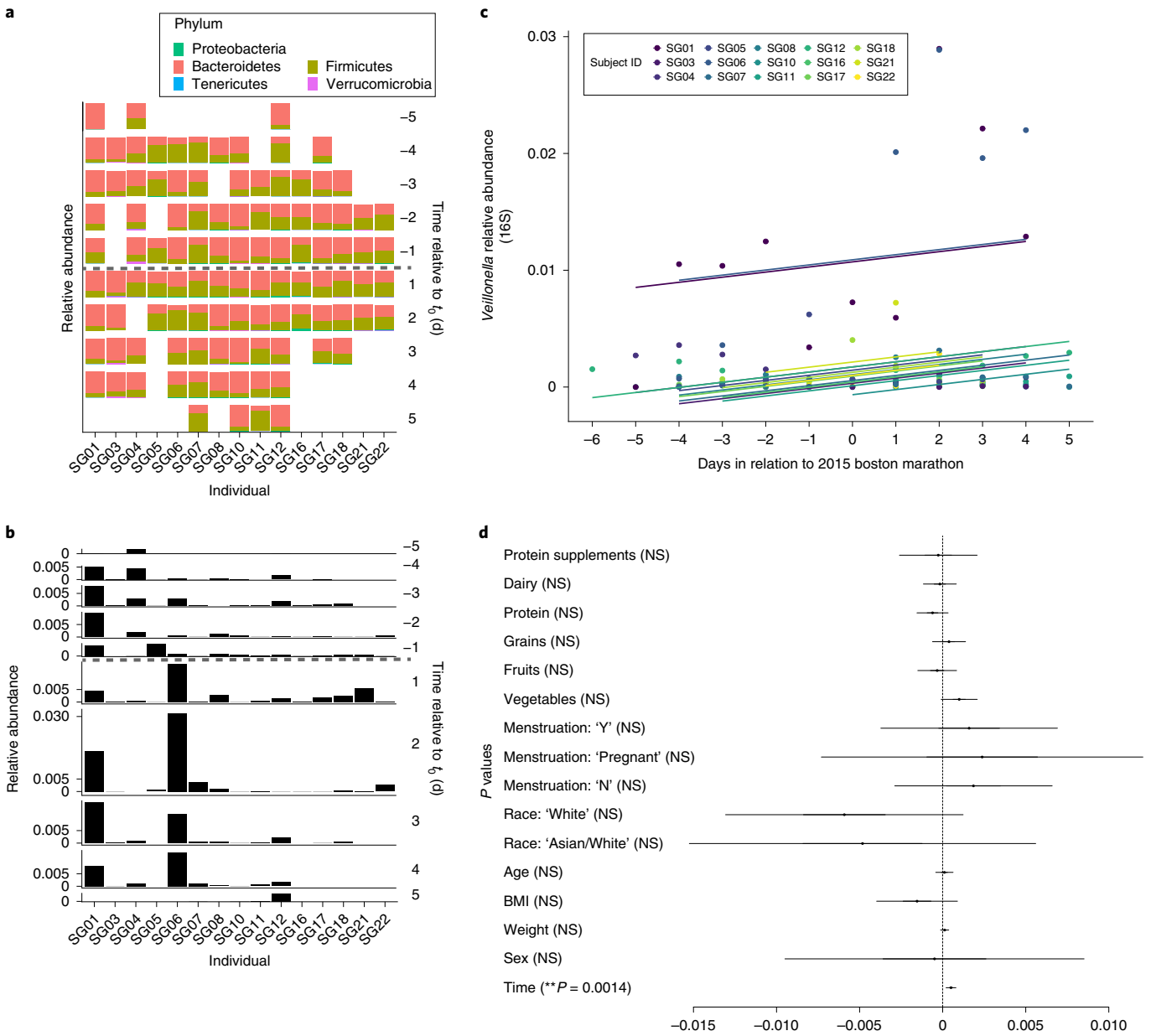

Fig. 1 | Gut *Veillonella* abundance is significantly associated with marathon running. a, Phylum-level relative abundance in marathon runners, partitioned by individual and time (−5 to +5 d in relation to running the marathon (t_0), where negative values are premarathon and positive values are postmarathon), showing few global differences in composition. **b**, *Veillonella* relative abundance at the genus level, partitioned by individual and time (−5 to +5 d in relation to running the marathon), showing that there is a significant difference in *Veillonella* relative abundance ($P = 0.02$, two-sided Wilcoxon rank-sum test with continuity correction; $n = 15$ individuals) between samples collected before and after exercise. **c**, GLMMs predicting longitudinal *Veillonella* relative abundance in the marathon participants. Differences in intercepts between fits for different marathon runners represent random effects. **d**, 95% confidence intervals for all of the fixed effects (coefficients) included in the GLMMs. All coefficients except time ($P = 0.0014$, Wald Z-test; time postmarathon corresponds to increased *Veillonella* relative abundance) were not significant (NS), suggesting that *Veillonella* blooms in runners correspond to exercise state and not other fixed effects ($n = 15$ individuals).

treatment/control crossover happening between weeks ($n = 32$ mice in total). *L. bulgaricus* was chosen as a control due its inability to catabolize lactate, thus mimicking the bacterial load but without impacting lactate metabolism[7]. The *Veillonella* strain used, *Veillonella atypica*, was directly isolated from one of the marathon runners. Mice were administered either *V. atypica* or *L. bulgaricus* and run to exhaustion 5 h later (Methods). In aggregate, on both sides of the crossover, mice gavaged with *V. atypica* had statistically significantly longer maximum run times than mice gavaged with *L. bulgaricus* ($P = 0.02$, paired *t*-test; Fig. 2a, Supplementary Table 3 and Extended Data Fig. 3). Both LOOCV and iterative permutation of labels were conducted as part of the GLMM analysis (Extended Data Fig. 3 and Methods). Per-mouse run times overlaid on the GLMM fits (Extended Data Fig. 4), as well as the difference between the maximum run times in *L. bulgaricus* versus *V. atypica* gavage, showed a distinction between 'responders' and 'non-responders' to *V. atypica* gavage (Extended Data Fig. 5). Mice treated with *V. atypica* ran, on average, 13% longer than the control group (Fig. 2a). Testing the significance of coefficients in the GLMM for their contribution to treadmill run time (Wald Z-test) showed that the

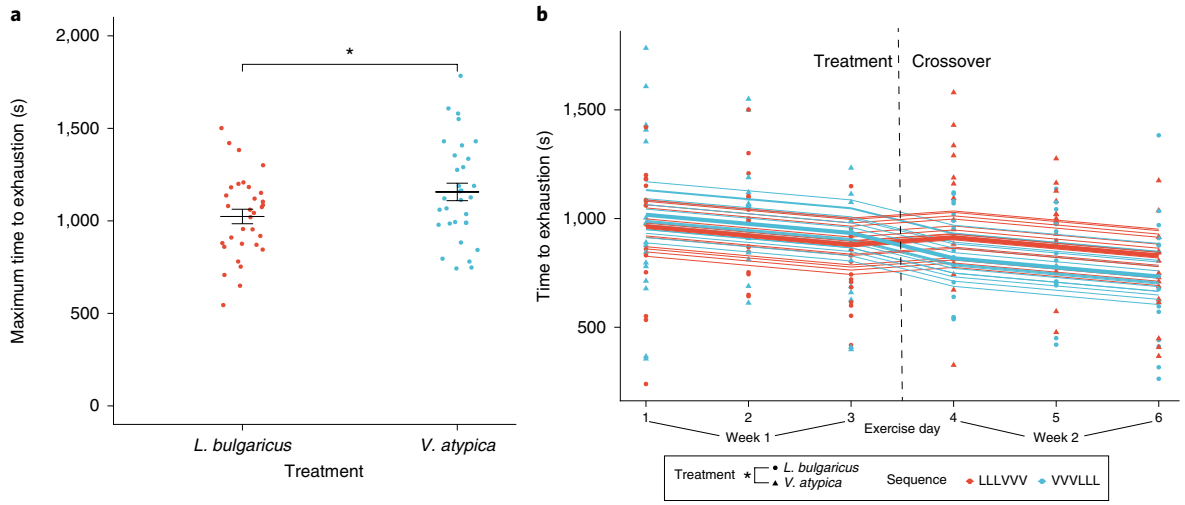

Fig. 2 | *V. atypica* gavage improves treadmill run time in mice. a, Mice gavaged with *V. atypica* had greater maximum run times per week than mice gavaged with *L. bulgaricus* in an AB/BA crossover trial. The graph shows the maximum run times out of 3 d of consecutive treadmill running for a given treatment (all mice switched treatments for the second week). The jitter plot shows each mouse as an individual point, with the central bar representing the mean and error bars representing s.e.m. ($n=32$). *$P=0.02$, as determined by two-sided paired *t*-test. **b**, GLMMs predicting run time in the 2-week AB/BA crossover trial. The colors of the lines (GLMM fits) and points (runs by an arbitrary mouse) represent the treatment sequence (in the legend, L represents *L. bulgaricus* and V represents *Veillonella atypica*). The shapes of the points represent the treatment at a given time point. These models incorporate both random effects (individual variation per mouse that manifests longitudinally) and fixed effects (treatment day, treatment sequence and treatment given). Visualization of all of the longitudinal data points with the GLMM predictions overlayed shows the effect of *V. atypica* increasing performance on both sides of the crossover when aggregated by treatment group (thick lines), as well as the trends for each of the 32 individual mice (thin lines). *$P=0.016$, as determined by Wald Z-test on model coefficients.

sequence effect was not significant ($P=0.758$), while treatment day ($P=0.031$; negative effect on run time) and *Veillonella* treatment ($P=0.016$; positive effect on run time) were significant (Fig. 2b and Extended Data Fig. 3). In a separate experiment, levels of inflammatory cytokines were quantified postexercise, and were significantly reduced in *Veillonella*-treated animals compared with *L. bulgaricus* or phosphate buffered saline (PBS) (Extended Data Fig. 6 and Supplementary Table 4). To assess changes in muscle physiology, the glucose transporter GLUT4 was quantified via western blot, but we observed no changes regardless of treatment (Extended Data Fig. 7).

To test whether our results would be replicated in an independent cohort of human athletes, we performed shotgun metagenomic sequencing of stool samples ($n=87$) from ultramarathoners and Olympic trial rowers both before and after exercise (Supplementary Table 5). Putative taxonomic abundances reproduced the previous 16S sequencing-based association with *Veillonella* (Extended Data Fig. 8)[8]. By utilizing novel algorithms that allow for cheap construction of metagenomic gene catalogs at a massive scale through the efficient use of cloud computing, we investigated phenotypic modulating effects of millions of microbial genes on athletes by building a sample ($n=87$) by gene ($n=2{,}288{,}155$) relative abundance matrix (Extended Data Figs. 8 and 9 and Methods)[9–13]. The inability of *Veillonella* to ferment carbohydrates, coupled with the high observed abundance of the lactate import permease in previously sequenced isolates, suggests that metabolic enzymes facilitating lactate breakdown are likely conserved[14]. Across the entire ultramarathon and rower cohorts, there exists a group of gene families with differential relative abundance pre- and postexercise (Extended Data Fig. 9), representing every step of the enriched methylmalonyl-CoA pathway ($P=0.00147$; Methods), degrading lactate into propionate, as assigned by Enzyme Commision (EC) ID numbers (Fig. 3a). Given the limited prevalence of the methylmalonyl-CoA pathway across lactate-utilizing microbes, this enrichment postexercise may implicate *Veillonella* in causing functional changes in the metabolic repertoire of the gut microbiome.

We verified strong production of acetate and propionate by performing mass spectrometry on spent media collected after growing three *Veillonella* strains isolated from the human athletes (*V. parvula*, *V. dispar* and *V. atypica*) in lactate-supplemented brain–heart infusion media (BHIL) and semi-synthetic lactate media (Fig. 4a, Supplementary Table 6 and Methods).

Veillonella species metabolize lactate into the short-chain fatty acids (SCFAs) acetate and propionate via the methylmalonyl-CoA pathway[15]. Lactate dehydrogenase—the enzyme responsible for the first step of lactate metabolism—is present in a phylogenetically diverse group of bacteria (Fig. 3b). Querying microbial isolate strain genome annotations from National Center for Biotechnology Information (NCBI) shows that, unlike *V. atypica*, many other microbes are theoretically capable of utilizing lactate through lactate dehydrogenase, but do not possess the full pathway to convert lactate into propionate (Fig. 3c). Other obligate anaerobes, such as *Anaerostipes caccae* and *Eubacterium hallii* commonly ferment lactate into butyrate via different pathways (Fig. 3c). *E. hallii* can also produce propionate; however, this has been demonstrated as a biotransformation of 1,2-propanediol, rather than a complete pathway from lactate to propionate. Of note, the reference genomes on NCBI for both *Veillonella dispar* and *Veillonella parvula* are not annotated to have the succinate-CoA transferase needed for propionate production to occur; this is likely to be due to an annotation error, as we validated the production of propionate via mass spectrometry on isolates of these species (Supplementary Table 6).

Taken together, these results show that not only is the genus *Veillonella* enriched in athletes after exercise but the metabolic pathway that *Veillonella* species utilize for lactate metabolism is also enriched. This result raises the possibility that systemic lactate resulting from muscle activity during exercise may enter the gastrointestinal lumen and become metabolized by *Veillonella*.

Next, we sought to determine whether systemic lactate is capable of crossing the epithelial barrier into the gut lumen, as this has not been demonstrated before to our knowledge. To investigate this, we

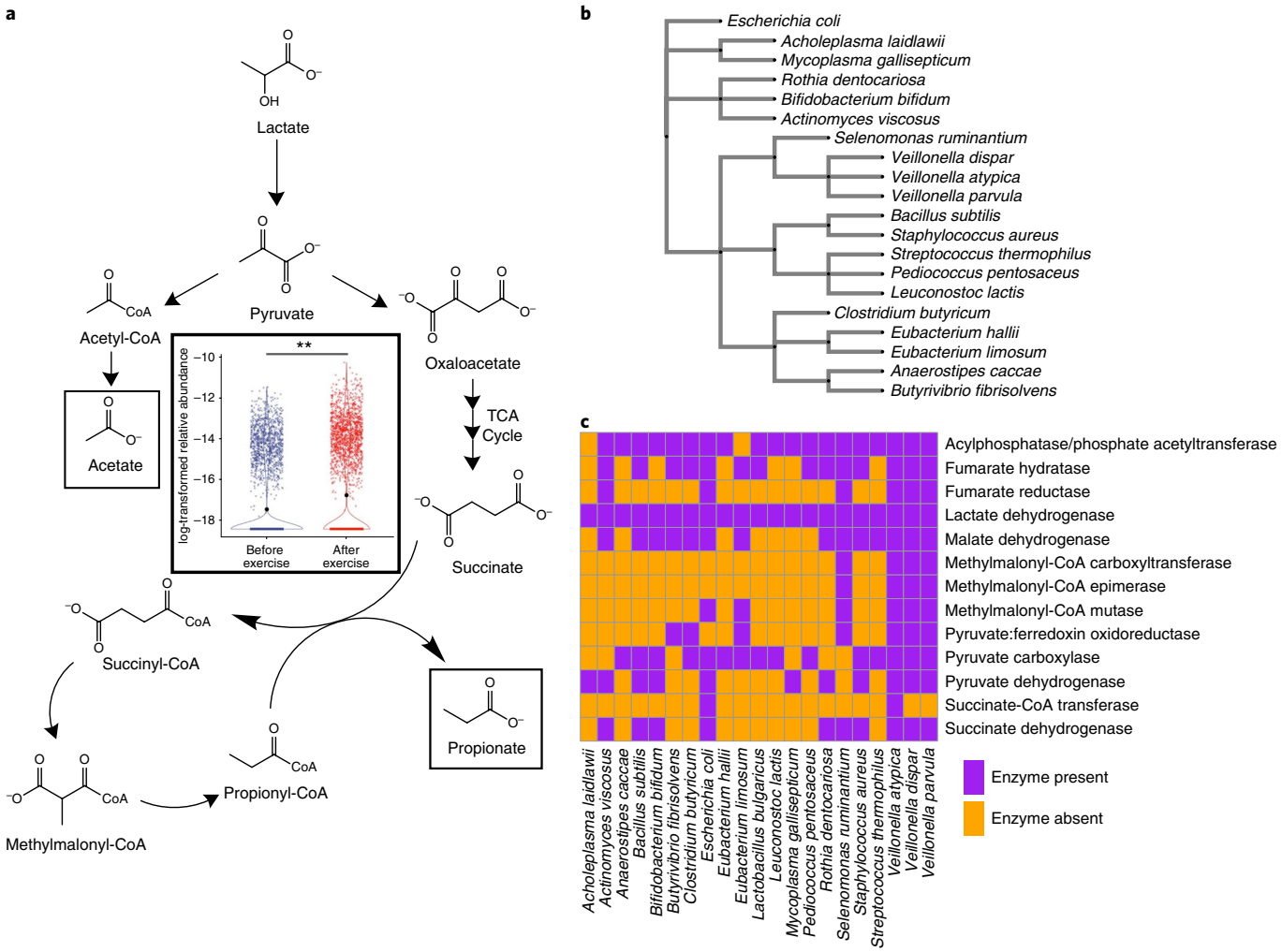

Fig. 3 | The athlete gut microbiome is functionally enriched for the metabolism of lactate to propionate postexercise. a, The methylmalonyl-CoA pathway, with conserved steps of the tricarboxylic acid (TCA) cycle abbreviated. Inset, significantly differentially expressed gene families within the methylmalonyl-CoA pathway in a pair of non-redundant gene catalogs created from metagenomic sequencing of athlete stool samples. The log-transformed relative abundance increases after exercise for every enzyme in the methylmalonyl-CoA pathway. $^{**}P = 0.00147$, as determined by two-sided Fisher's exact test ($n = 8$ enzymes in the pathway). Data are represented as a violin plot, which displays the distribution of data as a rotated kernel density distribution. **b**, Bacterial phylogenetic tree showing the diversity of microbes that have the ability to utilize lactate as a carbon source. **c**, Prevalence of enzymes in the methylmalonyl-CoA pathway that break down lactate into acetate and propionate in reference genomes from this representative subset of lactate-processing microbes.

performed tail vein injections of $^{13}C_3$ sodium lactate into mice colonized with either *V. atypica* or *L. bulgaricus*, and sacrificed them 12 min after injection. This time point was chosen because it was the earliest time at which we observed serum lactate levels return to baseline levels after tail vein injections in pilot experiments. At sacrifice, we immediately collected serum and plasma following cardiac puncture, and collected intestinal luminal contents by removing the colon and cecum from the mice and gently sampling the inner surface of the tissue. By performing liquid chromatography–mass spectrometry (LC-MS) on these tissues, we were able to identify $^{13}C_3$-labeled lactate present in both the serum and plasma, as well as in the lumen of the colons and ceca (Fig. 4b–d and Supplementary Table 7). We were unable to detect any $^{13}C_3$-labeled propionate in these tissues; however, the 12-min time point from tail vein injection to sacrifice is likely to have been insufficient time for labeled lactate crossing the gut barrier to be metabolized into propionate by the gut *Veillonella*.

As we have shown that serum lactate is capable of entering the intestinal lumen, we sought to determine whether *Veillonella* colonization may actively limit blood lactate levels by serving as a metabolic 'sink'. To test the capability of *Veillonella* to accelerate blood lactate clearance in vivo, we performed intraperitoneal injections of sodium lactate in mice colonized with either *V. atypica* or *L. bulgaricus*, and monitored blood lactate over time. Neither the basal nor the peak lactate levels between the treatment groups were significantly different (Extended Data Fig. 10 and Supplementary Table 8). The vast majority of lactate processing occurs in the liver[16], and although systemic lactate infiltrates the intestinal lumen, we did not observe a change in overall lactate clearance on inoculation with *Veillonella*.

Propionate has been shown to increase the heart rate and maximum rate of oxygen consumption, and to affect blood pressure in mice[17–19], as well as raise the resting energy expenditure and lipid oxidation in fasted humans[20]. To test whether the exercise-enhancing effects of *Veillonella* may be attributable at least in part to propionate, we performed intrarectal instillation of propionate in our mouse treadmill model. Propionate was introduced intrarectally rather than orally because colonic absorption provides a more direct route for propionate to reach the systemic circulation, mirroring the location of *Veillonella*-sourced propionate. Intrarectal propionate instillation ($n = 8$) compared with saline vehicle ($n = 8$) resulted in increased treadmill run times similar to those of *V. atypica* gavage

a

	Butyrate (μM)	Propionate (μM)	Pyruvate (μM)	Lactate (μM)	Acetate (μM)
V. atypica LM	19 ± 0.3***	10,611 ± 584**	4 ± 0.4***	431 ± 5.6***	92,432 ± 3,129**
L. bulgaricus LM	9 ± 0.5*	3 ± 1.5	32 ± 2.7	737 ± 45	4,985 ± 247**
LM alone	11 ± 0.1	4 ± 0.5	41 ± 0.4	851 ± 6.6	1,741 ± 12.2
V. atypica BHIL	69 ± 0.5*	2,286 ± 68*	NA	NA	4,149 ± 118*
BHIL alone	147 ± 4.1	160 ± 1.4	NA	NA	7,557 ± 30

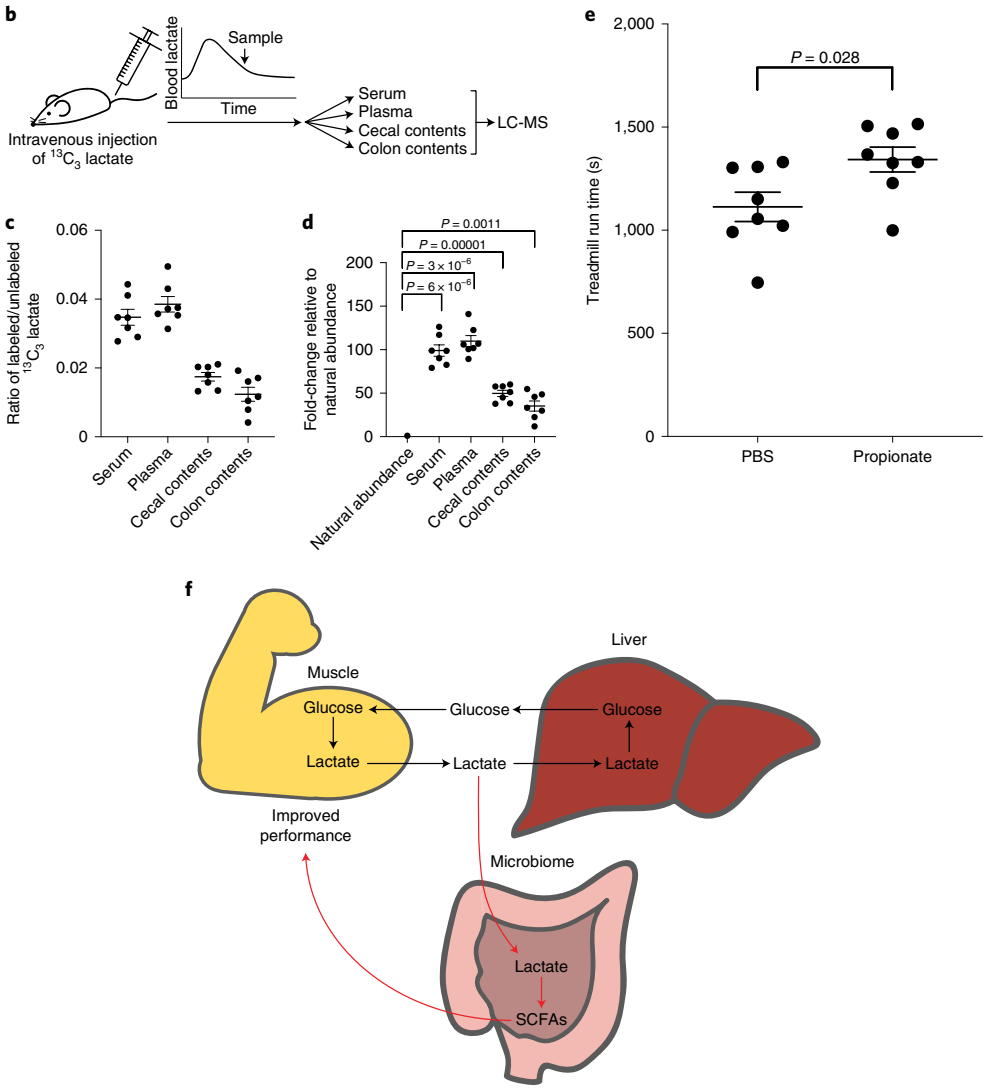

Fig. 4 | Serum lactate crosses the epithelial barrier into the gut lumen, and colorectal propionate instillation is sufficient to enhance treadmill run time. **a**, SCFAs detected in spent media after 48 h of growth with the indicated strain. LM, semi-synthetic lactate media; NA, not quantified. Each table entry shows the mean ± s.e.m. (BHIL, $n = 2$; LM, $n = 3$). *P* values from left to right, row by row were: ***$P = 0.0008$; **$P = 0.003$; ***$P = 4.4 \times 10^{-7}$; ***$P = 1.4 \times 10^{-6}$; **$P = 0.001$; *$P = 0.023$; **$P = 0.006$; *$P = 0.03$; *$P = 0.02$; and *$P = 0.015$, compared with the media control, as determined by two-sided Welch's *t*-test. **b**, Schematic of the $^{13}C_3$ flux-tracing experimental design. Mice were injected with $^{13}C_3$ sodium lactate, then sacrificed after 12 min. Serum and plasma were collected via cardiac puncture. Cecum and colon contents were collected by dissection. **c**, Abundance of $^{13}C_3$ lactate quantified relative to the abundance of unlabeled lactate. **d**, $^{13}C_3$ lactate abundance normalized to the expected natural abundance of $^{13}C_3$ lactate. The ratio of labeled/unlabeled lactate was quantified for experimental samples, as well as for the unlabeled lactate standard. Experimental samples are represented as the fold-change relative to the unlabeled standard. In **c** and **d**, each mouse sample is represented as an individual point, with the central bar representing the mean and error bars representing s.e.m. ($n = 7$). *P* values were determined by two-sided, one-sample *t*-test versus natural abundance. **e**, Intracolonic infusion of propionate improves the maximum run time in mice. The graph shows the maximum run times out of 3 d of consecutive treadmill running. The jitter plot shows each mouse as an individual point, with the central bar representing the mean and error bars representing s.e.m. ($n = 8$). The *P* value was determined by two-sided unpaired *t*-test. **f**, Proposed model of the microbiome–exercise interaction. Black arrows represent the well-known steps of the Cori cycle, where glucose is converted to lactate in the muscle, enters the liver via blood circulation, and is then is converted back to glucose in the liver via gluconeogenesis. Red arrows represent the steps proposed in this work. First, lactate produced in the muscle enters the intestinal lumen via the blood circulation. In the intestine, it acts as a carbon source for specific microbes, including *Veillonella* species. This causes the observed bloom in intestinal *Veillonella*, as well as the production of SCFA byproducts (predominantly propionate), which are taken up by the host via the intestinal epithelium. The presence of microbiome-sourced SCFAs in the blood improves athletic performance via an unknown mechanism. Together, this creates an addendum to the Cori cycle by converting an exercise byproduct into a performance-enhancing molecule, mediated by naturally occurring members of the athlete gut microbiome.

($P=0.03$; Fig. 4e). As in the *Veillonella* gavage experiments, we ran the same panel of inflammatory cytokines on serum taken 40 min after treadmill running, but found no significant differences in cytokine levels (Extended Data Fig. 6 and Supplementary Table 4). Therefore, the introduction of propionate into the colon is sufficient to result in an enhanced exercise phenotype via a mechanism that does not impact the inflammatory cytokines measured.

Coupling computational approaches, multi'omic data collection approaches and experimental validation looks promising as a method to approach unvalidated metagenomic associations that have been proposed in the past decade. Acting on this principle, we observed that: (1) *Veillonella* abundance increased in the gut microbiome postexercise in two independent cohorts of athletes; (2) the *Veillonella* methylmalonyl-CoA pathway is overrepresented in athlete metagenomic samples postexercise; (3) systemic lactate can cross the gut barrier into the lumen of the gut; (4) in a longitudinal AB/BA crossover study in mice, *Veillonella* inoculation improved treadmill performance; and (5) treadmill performance is improved in mice administered propionate via intracolonic infusion.

These data illustrate a model in which systemic lactate produced during exercise crosses to the gut lumen and is metabolized by *Veillonella* into propionate in the colon, which in turn serves to promote performance. Gut colonization of *Veillonella* may be augmenting the Cori cycle by providing an alternative lactate-processing method whereby systemic lactate is converted into SCFAs that re-enter the circulation (Fig. 4f). SCFAs are absorbed in the sigmoid and rectal region of the colon and enter circulation via the pelvic plexus, bypassing the liver and draining via the vena cava to reach the systemic circulation directly[21]. Microbiome-derived SCFAs then augment performance directly and acutely, suggesting that lactate generated during sustained bouts of exercise could be accessible to the microbiome and converted to these SCFAs that improve athletic performance.

In conclusion, we have shown that the microbiome may be a critical component of physical performance, and highlight the benefits derived from it. An important question is how this performance-facilitating organism first came to be more prevalent among athletes. We propose that the high-lactate environment of the athlete provides a selective advantage for colonization by lactate-metabolizing organisms such as *Veillonella*. Future studies are needed to help explain why there is an apparent preference for *Veillonella* and not any of the many other lactate-metabolizing organisms. *Veillonella* in the physically active host therefore serves as a potential example of a symbiotic relationship in the human microbiome.

Online content

Any methods, additional references, Nature Research reporting summaries, source data, statements of code and data availability and associated accession codes are available at https://doi.org/10.1038/s41591-019-0485-4.

Received: 21 May 2018; Accepted: 10 May 2019;
Published online: 24 June 2019

References

1. Gilbert, J. A. et al. Current understanding of the human microbiome. *Nat. Med.* **24**, 392–400 (2018).
2. Lax, S. et al. Longitudinal analysis of microbial interaction between humans and the indoor environment. *Science* **345**, 1048–1052 (2014).
3. Rothschild, D. et al. Environment dominates over host genetics in shaping human gut microbiota. *Nature* **555**, 210–215 (2018).
4. Dusko Ehrlich, S. & The MetaHIT Consortium. in *Metagenomics of the Human Body* 307–316 (Springer, 2011).
5. Petersen, L. M. et al. Community characteristics of the gut microbiomes of competitive cyclists. *Microbiome* **5**, 98 (2017).
6. Clarke, S. F. et al. Exercise and associated dietary extremes impact on gut microbial diversity. *Gut* **63**, 1913–1920 (2014).
7. Garvie, E. I. Bacterial lactate dehydrogenases. *Microbiol. Rev.* **44**, 106–139 (1980).
8. Truong, D. T. et al. MetaPhlAn2 for enhanced metagenomic taxonomic profiling. *Nat. Methods* **12**, 902–903 (2015).
9. Luber, J. M., Tierney, B. T., Cofer, E. M., Patel, C. J. & Kostic, A. D. Aether: leveraging linear programming for optimal cloud computing in genomics. *Bioinformatics* **34**, 1565–1567 (2017).
10. Li, D., Liu, C.-M., Luo, R., Sadakane, K. & Lam, T.-W. MEGAHIT: an ultra-fast single-node solution for large and complex metagenomics assembly via succinct de Bruijn graph. *Bioinformatics* **31**, 1674–1676 (2015).
11. Seemann, T. Prokka: rapid prokaryotic genome annotation. *Bioinformatics* **30**, 2068–2069 (2014).
12. Fu, L., Niu, B., Zhu, Z., Wu, S. & Li, W. CD-HIT: accelerated for clustering the next-generation sequencing data. *Bioinformatics* **28**, 3150–3152 (2012).
13. Qin, J. et al. A metagenome-wide association study of gut microbiota in type 2 diabetes. *Nature* **490**, 55–60 (2012).
14. Van den Bogert, B., Boekhorst, J., Smid, E. J., Zoetendal, E. G. & Kleerebezem, M. Draft genome sequence of *Veillonella parvula* HSIVP1, isolated from the human small intestine. *Genome Announc.* **1**, e00977-13 (2013).
15. Ng, S. K. C. & Hamilton, I. R. Carbon dioxide fixation by *Veillonella parvula* M4 and its relation to propionic acid formation. *Can. J. Microbiol.* **19**, 715–723 (1973).
16. Phypers, B. & Pierce, J. M. T. Lactate physiology in health and disease. *Contin. Educ. Anaesth. Crit. Care Pain* **6**, 128–132 (2006).
17. Kimura, I. et al. Short-chain fatty acids and ketones directly regulate sympathetic nervous system via G protein-coupled receptor 41 (GPR41). *Proc. Natl Acad. Sci. USA* **108**, 8030–8035 (2011).
18. Pluznick, J. A novel SCFA receptor, the microbiota, and blood pressure regulation. *Gut Microbes* **5**, 202–207 (2014).
19. Pluznick, J. L. et al. Olfactory receptor responding to gut microbiota-derived signals plays a role in renin secretion and blood pressure regulation. *Proc. Natl Acad. Sci. USA* **110**, 4410–4415 (2013).
20. Chambers, E. S. et al. Acute oral sodium propionate supplementation raises resting energy expenditure and lipid oxidation in fasted humans. *Diabetes Obes. Metab.* **20**, 1034–1039 (2018).
21. Araghizadeh, F. & Abdelnaby, A. in *Colorectal Surgery* (eds Bailey, H. R., Billingham, R. P., Stamos, M. J. & Snyder, M. J.) 3–17 (Elsevier Health Sciences, 2012).

Acknowledgements

This work was funded by the Synthetic Biology platform at the Wyss Institute for Biologically Inspired Engineering at Harvard University; National Institutes of Health (NIH)/National Human Genome Research Institute grant T32 HG002295 (to J.M.L.; principal investigator: P. J. Park); NIH/National Institute of Diabetes and Digestive and Kidney Diseases grant T32 DK007260 (to T.A.C.; principal investigator: T. K. Blackwell); a National Science Foundation Graduate Research Fellowship Program fellowship (to J.M.L.); National Library of Medicine BIRT grant T15LM007092 (to B.T.T.); an AWS Research Credits for Education Grant (to J.M.L. and A.D.K.); a Smith Family Foundation Award for Excellence in Biomedical Research (to A.D.K.); an American Diabetes Association Pathway to Stop Diabetes Initiator Award (to A.D.K.) and NIH/National Institute of Diabetes and Digestive and Kidney Diseases Diabetes Research Center grant P30DK036836-30 (to J.M.L., T.A.C., T.M., B.T.T., L.-D.P., Z.Y., M.C.W., S.L. and A.D.K.; principal investigator: G. L. King). We acknowledge C. J. Patel and S. R. Stein for statistical advice, and S. Softic for assistance with tail vein injections.

Author contributions

J.S., G.M.C. and A.D.K. conceived the project. J.S. collected the athlete samples and metadata. J.M.L. performed the computational analysis and modeling, with assistance from T.A.C., M.C.W., R.C.W., B.T.T., Z.Y. and M.W.H. T.A.C. designed and performed the model organism experiments, with assistance from J.M.L., T.M., A.T., L.-D.P., M.C.W., S.P. and S.L. J.A.-P. and C.B.C. processed the metabolomic samples. J.M.L., T.A.C. and A.D.K. wrote the manuscript. G.M.C. and A.D.K. supervised the project.

Competing interests

J.S. and G.M.C. are co-founders of FitBiomics. Along with A.D.K., they hold equity in FitBiomics.

Additional information

Extended data is available for this paper at https://doi.org/10.1038/s41591-019-0485-4.

Supplementary information is available for this paper at https://doi.org/10.1038/s41591-019-0485-4.

Reprints and permissions information is available at www.nature.com/reprints.

Correspondence and requests for materials should be addressed to G.M.C. or A.D.K.

Peer review information: Joao Monteiro was the primary editor on this article and managed its editorial process and peer review in collaboration with the rest of the editorial team.

Publisher's note: Springer Nature remains neutral with regard to jurisdictional claims in published maps and institutional affiliations.

Methods

Participation recruitment. All study participants were recruited following a Sports Genomics protocol (number IRB15-0869) approved by the Institutional Review Board of the Wyss Institute for Biologically Inspired Engineering. Each participant read and signed a consent form before study enrollment, and we have complied with all of the relevant ethical regulations.

Sample collection, extraction and library preparation. For the collection of materials, study participants were provided with a 15 ml falcon tube with a 1 ml pipette tip inserted inside. Participants were instructed to dip the pipette tips into soiled toilet tissue, then place them back into the tubes and label the tubes with the date and time of collection. Samples were kept at 4 °C for short-term storage until sample pickup, at which point they were immediately placed onto dry ice, then transferred to a −80 °C freezer for long-term storage.

Fecal samples were thawed on ice and resuspended in 2–5 ml of PBS, 250 µl of which was used for DNA extraction using the Mo Bio PowerSoil high-throughput DNA extraction kit, following the manufacturer's protocol. For 16S rDNA library construction, 1–5 µl of purified DNA was used for PCR amplification of the V4 variable region using Q5 Hot Start Polymerase (NEB). Primers were adapted from the Earth Microbiome Project (http://www.earthmicrobiome.org/), attaching Illumina paired-end adapters (forward: CTT TCC CTA CAC GAC GCT CTT CCG ATC TGT GCC AGC MGC CGC GGT AA; reverse: GGA GTT CAG ACG TGT GCT CTT CCG ATC TGG ACT ACH VGG GTW TCT AAT). Illumina barcodes were added to libraries during a second PCR step (forward: AAT GAT ACG GCG ACC ACC GAG ATC TAC ACT CTT TCC CTA CAC GAC GCT C; reverse: CAA GCA GAA GAC GGC ATA CGA GAT GTG ACT GGA GTT CAG ACG TGT GCT C) and end products were purified via column chromatography (Zymo Research). Individual libraries were quantified and normalized for sequencing using the Quant-iT PicoGreen reagent (Thermo Fisher Scientific). For whole-genome shotgun library construction, 1 ng of purified DNA was used for Illumina's Nextera XT Tagmentation kit, following the manufacturer's protocol. Libraries were submitted to the Harvard Biopolymers core sequencing facility for bioanalyzer quality control and 150-base pair paired-end sequencing reads using either the Illumina MiSeq or HiSeq 2500 system (high output mode) for 16S rDNA and shotgun analysis, respectively.

Metadata collection. Each study participant was provided with a questionnaire to collect health, dietary and athletic background information (adapted from The American Gut; http://americangut.org/). Additionally, for each sample collection, study participants filled out a daily annotation sheet to collect dietary, exercise and sleep information.

16S analysis. Each subject provided fecal samples on a daily basis, up to one week before and one week after the marathon (controls did not run in the marathon but provided fecal samples). Next, we extracted genomic DNA from these samples and performed 16S rDNA amplicon sequencing, followed by bioinformatic analysis, to obtain genus-level resolution of bacteria in each individual's microbiome (Supplementary Tables 1 and 2).

16S reads were processed with the DADA2 pipeline and phyloseq[22,23]. Default settings were used for filtering and trimming. Built-in training models were utilized to learn error rates for the amplicon dataset. Identical sequencing reads were combined through DADA2's dereplication functionality, and the DADA2 sequence–variant inference algorithm was applied to each dataset. Subsequently, paired-end reads were merged, a sequence table was constructed, taxonomy was assigned, and abundance was calculated at all possible taxonomic levels.

16S mixed-effects modeling in the human cohort. We constructed a series of GLMMs to predict *Veillonella* relative abundance in the marathon participants from both random effects (individual variation per athlete that manifests longitudinally) and fixed effects (United States Department of Agriculture (USDA) MyPlate consumption categories, protein powder supplementation, menstruation status, race, time, body mass index (BMI), weight, gender and age).

The longitudinal nature of the microbiome sampling, coupled with the unique lifestyles of athletes, means that diet, physical characteristics, age, gender, ethnicity and the menstrual cycle could potentially confound the association between postmarathon state and *Veillonella* relative abundance[24,25]. As some food compounds can selectively increase the relative abundance of *Veillonella*, 1,267 meal records logging every instance of food consumption over the course of the study (Supplementary Table 1) were quantified according to USDA MyPlate and associated with daily microbiome samples. LOOCV was performed for the GLMM analysis where the *P* value for the time coefficient was calculated for all permutations of eliminating one athlete, which revealed a general trend of no individual athlete driving significance, with one minor outlier (Extended Data Fig. 1; Wald Z-tests). To ensure that an arbitrary shuffling of participant labeling would not yield significant results, the GLMM was trained 1,000 times on input data with permuted labels, which generated uniformly distributed *P* values and showed the significance of the original labeling (Extended Data Fig. 1; Wald Z-tests). Thus, the observed significance of the association between *Veillonella* relative abundance and pre- and postmarathon state is likely not confounded by any fixed effects. To test whether *Veillonella* has any phenotypic impact on running ability, we next introduced *Veillonella* to mice in a treadmill experiment.

Modeling of 16S *Veillonella* relative abundance for athletes participating in the marathon was done with the R nlme package[26]. A total of 1,267 meal records logging every instance of food consumption over the course of the study were quantified according to USDA MyPlate and associated with daily 16S samples by a nutritionist. Relative abundance was first modeled as:

$$\text{Abundance} = \beta_0 + \beta_{\text{time}} + \beta_{\text{sex}} + \beta_{\text{weight}} + \beta_{\text{BMI}} + \beta_{\text{age}} + \beta_{\text{race}} + \beta_{\text{menstruation}} + \beta_{\text{vegetables}} + \beta_{\text{fruits}} + \beta_{\text{grains}} + \beta_{\text{protein}} + \beta_{\text{dairy}} + \beta_{\text{dietary protein supplementation}}$$

Subsequently, a second model was generated that included interaction terms of time:vegetables and time:menstruation. Significance was calculated for all of the coefficients included in the GLMM with Wald Z-tests (default calculation in the library utilized). Coefficients were created with the coefplot2 package[27].

The code for the two models is provided below.

```
Model_1 < -lme(Veillonella~time + sex + weight + BMI + age + race
+ menstruation + vegetables + fruits + grains + protein + dairy + dietary_protein_
supp,random = ~1|subjectID,data = marathon16S)
Model_2 < -lme(Veillonella~time + sex + weight + BMI + race + menstruation
+ vegetables + fruits + grains + protein + dairy + dietary_protein_
supp + time:vegetables + time:menstruation,random = ~1|subjectID,
data = marathon16S)
```

Model predictions overlayed on the underlying data were visualized with the ggplot2 R package[28].

Model results were validated with both LOOCV and permutation testing on shuffled labels.

Preparation of bacteria for gavage. *V. atypica* and *L. bulgaricus* were grown in 250 ml BHIL (10 ml of 60% sodium lactate per liter) and MRS broth, respectively. The optical density measured at a wavelength of 600 nm (OD_{600}) was monitored and at an optical density of 0.4–0.6, cells were pelleted by refrigerated centrifugation at 5,000*g* for 10 min. The pellet was washed in PBS and resuspended in 2 ml residual PBS. Aliquots of 100 µl were frozen at −80 °C and the numbers of colony-forming units (c.f.u.) per ml were measured by serial dilution onto BHIL agar plates. *V. atypica* was gavaged in wild-type C57BL/6 mice to determine viability and transit time through the gastrointestinal tract, observing peak viable bacterial c.f.u. counts in fecal pellets 5 h after gavage.

Treadmill crossover experiment. Animal research was approved by the Joslin Diabetes Center Institutional Animal Care and Use Committee and we complied with all of the relevant ethical regulations. For the treadmill experiments, 8- to 12-week-old CL57BL/6 mice ($n = 32$) were acclimated to treadmilling with two bouts of 30 min of 5 m min^{-1} walking, split over two consecutive days. For exhaustion measurements, mice were fasted for 7 h before exercise. Then, 6 h before exercise, mice were gavaged with 200 µl of 2.5% sodium bicarbonate to neutralize the stomach contents, and 20 min after the first gavage, mice were gavaged 200 µl of either *V. atypica* or *L. bulgaricus*, prepared as above and normalized to 5×10^9 c.f.u. ml^{-1}. Next, 5 h postgavage, mice were run on the treadmill, starting at 5 m min^{-1} and increasing the speed by 1 m min^{-1} every minute until exhaustion. The time of exhaustion was recorded for every animal, defined as a mouse failing to return to the treadmill from the rest platform after three consecutive attempts to continue running. This protocol was repeated for two more days, followed by 4 d of rest and 3 d of crossover treatment. On the first day of treatment, serum was collected 40 min postexhaustion via a tail vein bleed and measured via Ciraplex multiplex mouse cytokine assay (Aushon Biosystems).

Treadmill run time mixed-effects modeling. Despite the high number of mice utilized in the AB/BA crossover experiment, comparisons of raw run times in this context could be confounded both by carryover effect (modeled as a sequence effect) inherent in the longitudinal study design, as well as unavoidably high intermouse variation. To account for this, we constructed a series of GLMMs predicting run time (Methods). These models incorporate both random effects (individual variation per mouse that manifests longitudinally) and fixed effects (treatment day, treatment sequence and treatment type given). Modeling was conducted with the R nlme package[26]. Visualization of coefficients was conducted using the coef2plot R package[27]. Visualization of predictions overlayed on data was conducted using the R ggplot2 package[28].

Visualization of all longitudinal data points with the GLMM predictions overlayed showed both the effect of *V. atypica* increasing performance on both sides of the crossover when aggregated by treatment group (thick lines), and the trends for each of the 32 individual mice (thin lines) (Fig. 2b). LOOCV was performed for the GLMM analysis where the *P* value for the *V. atypica* treatment coefficient was calculated for all permutations of eliminating one mouse, which revealed that no individual mice were driving significance (Extended Data Fig. 3; Wald Z-tests). To ensure that an arbitrary shuffling of mouse labeling would not yield significant results, the GLMM was trained 1,000 times on input data with permuted labels, which generated uniformly distributed *P* values and showed the significance of the original labeling (Extended Data Fig. 3; Wald Z-tests). This longitudinal modeling approach allows us to interpret that, as the treadmill runs were conducted back to back each week on subsequent days, the mice in aggregate

had decreasing run times as the time to exhaustion decreased (visible as a slope of predictions in Fig. 2b), while *V. atypica* treatment independently increased run times (visible as the crossover of predictions showing the *Veillonella* treatment group having longer times to exhaustion on both sides of the crossover in Fig. 2b). To identify possible biological mechanisms for the *Veillonella* effect, we quantified levels of various inflammatory cytokines in the blood immediately following the treadmill run. We observed that several proinflammatory cytokines, including tumor necrosis factor-α and interferon-γ, were significantly reduced in *V. atypica*-treated mice compared with both the baseline and the control treatment (Extended Data Fig. 6 and Supplementary Tables 4 and 13). In a separate experiment, we quantified levels of the muscle glucose transporter GLUT4 to assess the effects on muscle physiology, but found no difference between the *V. atypica* treatment and control (Extended Data Fig. 7). Together, taking into account intermouse variation, the longitudinal study design and the possible carryover effects of an AB/BA crossover trial, *V. atypica* treatment causes substantial increases in treadmill run time in mice.

The models were constructed to predict treadmill run time in the AB/BA crossover experiment to include the treatment effect of *Veillonella*, period effects (time of treatment), carryover effects due to the treatment crossover, and effects for naturally occurring mouse variation. In general, we can model expected run time as:

Sequence: *V. atypica* → *L. bulgaricus* Week 1: $\mu+\pi_1+\alpha_A$ Week 2: $\mu+\pi_2+\alpha_B+\lambda_A$

Sequence: *L. bulgaricus* → *V. atypica* Week 1: $\mu+\pi_1+\alpha_B$ Week 2: $\mu+\pi_2+\alpha_A+\lambda_B$

Where α_A and α_B are treatment effects, λ_A and λ_B are carryover effects, and π_1 and π_2 are period effects.

We initially attempted to model carryover effect as a sequence effect or a period-specific treatment effect (interaction term). The R code for the models is provided below:

```
Model_1 < -lme(seconds_run~treatment + sequence + period,random
= ~1|subject,data = datain)
Model_2 < - lme(seconds_run~treatment*period,random
= ~1|subject,data = datain)
```

By gauging the correlation of coefficients, we selected model_1 for the analysis in Fig. 2.

Metagenomic analysis. All of the steps in the processing of raw metagenomic data were done utilizing the Aether package[9]. Raw reads were de novo assembled using megahit[10]. Open reading frames and annotations were generated using prokka[11]. A gene family catalog was generated from the called open reading frames at 95% identity utilizing the CD-HIT software package[12]. A raw abundance count matrix was generated utilizing the gene family catalog, Bowtie 2 and SAMtools[29,30]. The raw abundance count matrix was normalized both by sample and by gene length[13]. Metabolic pathways were queried using MetaCyc, and EC IDs were pulled from prokka annotations[11,31]. R was utilized to perform the majority of statistical tests, with the exception of pairwise analysis of variance (ANOVA) tests, for which the SciPy library in Python was used[32]. Root mean square error calculations were performed using the plotrix package[33].

MetaPhlAn2 taxonomy in metagenomics data. Putative taxonomic abundances were calculated with MetaPhlAn2 (ref. [8]) and found to have the same association between *Veillonella* and exercise status as the previous marathon runner results ($P=0.03$; Extended Data Fig. 8).

Annotations. To compare trends in the aggregate microbiome with the metabolic processes of microbes that had elevated 16S abundance in the previous experiment, a pairwise ANOVA was performed on all ~2.3 million genes in the catalog to look for significant differences before and after exercise. A total of 396 gene families with unique annotations showed statistically different relative abundance ($P<0.005$). While false discovery rate correction did not yield significant individual genes, of these 396 gene families, 391 share functional annotations with the reference assemblies of the *V. atypica*-type strain on NCBI. Of the significant genus-level results from the 16S data, *Veillonella* has extremely high-quality assemblies of cultured isolates.

Significant alleles are present in each of the 87 samples (Extended Data Fig. 8). Interestingly, when all 396 significant alleles are segregated by exercise state and sample, discordant shifts of relative abundance are observed (Extended Data Fig. 8). This suggests that changes in global microbiome function are associated with *Veillonella* abundance, and that conserved *Veillonella* genes may generally play metabolic roles.

Comparative genomics. Genome annotations were retrieved from NCBI reference genomes. Phylogenetic trees were generated from NCBI taxonomy and visualized with phylo.io[34]. Heat maps were generated with the pheatmap package in R[35].

Gene catalog creation. Raw reads were processed and de novo assembled into 4,802,186 contigs[9,10]. A total of 4,792,638 total open reading frames were called, which were subsequently clustered into 2,288,155 gene families with a threshold of 95% identity to create a gene catalog alongside putative annotations assigned by homology[11,12]. Of these gene families, 801,307 were assigned annotations and 1,486,948 were putatively classified as hypothetical proteins. Comparing annotation state versus gene family size yields the expected result that larger families, which are likely to be present in more microbes, tend to have many more annotations (Extended Data Fig. 8). Raw reads were then aligned back to the gene catalog to create a raw count abundance matrix[29,30]. This matrix was normalized both per sample and by gene length to create a relative abundance matrix[13].

Pathway elucidation. Reactions involved in the breakdown of lactate to both propionate and acetate were manually associated with EC IDs using MetaCyc[31].

In vitro growth and SCFA analysis. *Veillonella* species (*V. dispar*, *V. parvula* and *V. atypica*) were isolated and purified from several study participants and grown in three different media compositions: (1) BHIL (10 ml of 60% sodium lactate per liter); (2) MRS broth (BD) supplemented with lactate (10 ml of 60% sodium lactate per liter); and (3) semi-synthetic lactate medium (per liter: 5 g bacto yeast extract, 0.75 g sodium thioglycolate, 25 ml basic fuchsin and 21 ml 60% sodium lactate (pH 7.5)). *Veillonella* species were inoculated into each medium, under anaerobic conditions, and allowed to grow for 48 h to reach the stationary phase. After 48 h, bacteria were pelleted and supernatants were collected for lactate and SCFA measurements. Approximately 10 µl of supernatant was used to measure the lactate via the Lactate Scout (lactate.com). The remaining supernatants were frozen at −80 °C, then submitted to the Harvard Small Molecule Mass Spectrometry core facility for butyrate, propionate and acetate quantitative analysis.

SCFAs identified from the mass spectrometry in all three media conditions corresponded with the propionate end product suggested by the metagenomic results. Acetate was not observed in MRS or BHIL, likely due to high existing concentrations in the media making the forward reaction thermodynamically unfavorable. However, acetate production was observed in semi-synthetic lactate media (Supplementary Table 7).

$^{13}C_3$-lactate flux tracing. Ten-week-old C57BL/6 mice were treated with sodium bicarbonate followed by 10^9 c.f.u. of either *V. atypica* ($n=4$) or *L. bulgaricus* ($n=4$), prepared as above. Then, 20% *w/w* $^{13}C_3$ sodium lactate (Cambridge Isotope Laboratories) was diluted to a concentration of 400 mM in PBS. Mice were injected with 100 µl intravenously via the tail vein and, after 9 min, anesthetized with isoflurane. One mouse treated with *V. atypica* was unable to be injected due to vein clamping and had to be removed. Next, 10 min postinjection, anesthesia was confirmed via foot pinch and mice were sacrificed via cardiac puncture. Whole blood was divided into two samples to obtain both serum and plasma. These were flash frozen in liquid nitrogen at 12 min postinjection and stored at −80 °C.

Immediately following cardiac puncture, mice were dissected to remove the colon and cecum, and the contents were removed by squeezing with sterilized forceps into preweighed tubes. The contents were immediately flash frozen in liquid nitrogen. The timing varied slightly, but this was done between 17 and 19 min postinjection.

Samples were analyzed for lactate and propionate by the Broad Institute Metabolomics Platform. LC-MS metabolomics were performed as previously described[36]. LC-MS traces were identified and integrated to quantify the presence of $^{13}C_0$- and $^{13}C_3$-lactate isotopes.

Colorectal propionate instillation. Treadmilling followed the same protocol as above. Mice were fasted 7 h before exercise to normalize their metabolic profiles. Some 30 min before exercise, mice were treated with 200 µl of either PBS vehicle alone ($n=8$) or 150 mM sodium propionate in PBS ($n=8$), using a flexible gavage needle to introduce 200 µl of solution into the colon. Mice were then run to exhaustion as above. This protocol was repeated for three consecutive days. On the first day of treatment, serum was collected 40 min postexhaustion via tail vein bleed and measured using the Ciraplex multiplex mouse cytokine assay (Aushon Biosystems).

Lactate clearance. To measure the lactate clearance rate, mice were first fasted for 7 h before measurement to stabilize the basal lactate levels. Then, 5 h before measurement, mice were treated with sodium bicarbonate followed by 10^9 c.f.u. of either *V. atypica* or *L. bulgaricus*, prepared as above ($n=8$). Next, 30 min before measurement, mice were weighed and individually caged, and a baseline blood lactate reading was taken using a Lactate Scout meter. Mice were administered sodium lactate via intraperitoneal injection with a dose of 750 mg kg^{-1}, prepared as a 75 mg ml^{-1} solution of sodium lactate in pH 7.0 PBS. Blood lactate levels were monitored with a Lactate Scout meter at 5, 15, 25, 35 and 45 min postinjection.

Statistics. For Fig. 1a,b, Wilcoxon rank-sum tests with continuity correction were used to investigate differences in taxonomic composition before and after exercise. The mean *Veillonella* abundance was 0.9 orders of magnitude greater 1 d postexercise compared with 1 h before exercise.

For Fig. 1c,d, longitudinal data were modeled using a GLMM approach. In our model, the random effect was individual variation per marathon runner. Fixed effects are shown in Fig. 1d. An advantage of this type of statistical analysis is that it can account for the large variation between marathon participants in this type of study.

To determine statistical significance, a Wald Z-test was used to assign *P* values to coefficients in the GLMM. No outliers were removed in this analysis.

For Fig. 2a, each animal was treated with both *V. atypica* and *L. bulgaricus* as part of the AB/BA crossover. Because all 32 animals were treated twice and compared between treatments, the *P* value was generated using a paired *t*-test ($P=0.022$). The normality assumption was assessed via Shapiro–Wilk's normality test ($P=0.67$), validating the use of the *t*-test.

For Fig 2b, longitudinal data were modeled using a GLMM approach. In our model, the random effect was individual variation per mouse. Fixed effects were treatment effect, period effect (the time point at which measurements were made) and carryover/sequence effect (if the order of treatments in the crossover affected later results). An advantage of this type of statistical analysis is that it can account for the large variation between mice in this type of study.

Figure 2b shows the number of seconds run until exhaustion at six time points, with each of the 32 mice having one measurement per time point. For each treatment order (LLLVVV and VVVLLL), the GLMM was fitted both to each individual mouse (skinny blue and red lines; note that these are all parallel for mice in the same treatment order—the space between these lines represents the 'random effect' of natural variation between mice) and all mice with the same treatment order (thick blue and red lines).

To determine statistical significance, a Wald Z-test was used to assign *P* values to coefficients in the GLMM. No outliers were removed from this analysis.

For Fig. 3a and Extended Data Fig. 9, *P* values for individual genes were generated utilizing pairwise ANOVA comparing the relative abundance before and after exercise. Non-significant families were associated with homologs common in other microbes that do not change in abundance. To determine the significance of potential over-representation, 1,000 global EC IDs were randomly selected, and mean differences in relative abundance between samples taken before and after exercise were calculated. These EC IDs were used to construct an odds table to determine the probability of having a set of eight selected EC IDs with increases in mean gene level relative abundance after exercise. This calculation determined that the relative abundance changes in Fig. 3b–i are significant ($P=0.00147$, Fisher's exact test for count data).

For Supplementary Table 1, *P* values were generated using Welch's *t*-test (unequal variances *t*-test).

For Fig. 4d, *P* values were generated using a one-sample *t*-test. Ratios of labeled/unlabeled lactate from samples were compared with the expected ratio determined mathematically. Each sample was independently compared with the expected ratio, then multiple hypothesis correction was performed using the false discovery rate correction method of Benjamini and Hochberg (serum, $P=0.00001$; plasma, $P=0.00001$; cecum content, $P=0.00001$; colon content, $P=0.001$).

For Fig. 4e, the *P* value ($P=0.028$) was generated using Welch's *t*-test (unequal variances *t*-test).

Reporting Summary. Further information on research design is available in the Nature Research Reporting Summary linked to this article.

Data availability

All raw sequencing data have been uploaded to NCBI and SRA in the form of the BioProjects PRJNA472785 (16S) and PRJNA472768 (MGX). These are linked to associated BioSamples, which in turn are linked to the paired-end read files in the SRA, and correspond to the metadata in the Supplementary Information files.

Code availability

Unless otherwise noted, all plots were generated in R version 3.4.1 with the ggplot2, dplyr, scales, grid and reshape2 packages[28,37–40]. Large-scale data analysis was done on AWS, utilizing machines running Ubuntu 16.04. Data curation methods were coded in python version 2.7.12. The Aether package utilized for analysis is available at https://github.com/kosticlab/aether.

References

22. Callahan, B. J. et al. DADA2: high-resolution sample inference from Illumina amplicon data. *Nat. Methods* **13**, 581–583 (2016).
23. McMurdie, P. J. & Holmes, S. phyloseq: an R package for reproducible interactive analysis and graphics of microbiome census data. *PLoS ONE* **8**, e61217 (2013).
24. Jurkowski, J. E., Jones, N. L., Toews, C. J. & Sutton, J. R. Effects of menstrual cycle on blood lactate, O_2 delivery, and performance during exercise. *J. Appl. Physiol.* **51**, 1493–1499 (1981).
25. Pimentel, G. et al. Blood lactose after dairy product intake in healthy men. *Br. J. Nutr.* **118**, 1070–1077 (2017).
26. Pinheiro, J., Bates, D., DebRoy, S., Sarkar, D & R Development Core Team. nlme: Linear and nonlinear mixed effects models. R package version 3.1-117 http://CRAN.R-project.org/package=nlme (2014).
27. Bolker, B. M. coefplot2: Coefficient Plots. R package version 0.1.3.3 http://r-forge.r-project.org/R/?group_id=1059 (2012).
28. Wickham, H. & Chang, W. ggplot2: An implementation of the grammar of graphics. R package version 1 http://CRAN.R-project.org/package=ggplot2 (2015).
29. Langmead, B. & Salzberg, S. L. Fast gapped-read alignment with Bowtie 2. *Nat. Methods* **9**, 357–359 (2012).
30. Li, H. et al. The Sequence Alignment/Map format and SAMtools. *Bioinformatics* **25**, 2078–2079 (2009).
31. Caspi, R. et al. The MetaCyc database of metabolic pathways and enzymes and the BioCyc collection of pathway/genome databases. *Nucleic Acids Res.* **38**, D473–D479 (2010).
32. Jones, E et al. SciPy: Open source scientific tools for python, http://www.scipy.org/ (2001).
33. Lemon, J. et al. plotrix: Various plotting functions. R package version 3.7 https://cran.r-project.org/package=plotrix (2007).
34. Robinson, O., Dylus, D. & Dessimoz, C. Phylo.io: interactive viewing and comparison of large phylogenetic trees on the web. *Mol. Biol. Evol.* **33**, 2163–2166 (2016).
35. Kolde, R. Pheatmap: pretty heatmaps. R package version 61 (2012).
36. Fujisaka, S. et al. Diet, genetics, and the gut microbiome drive dynamic changes in plasma metabolites. *Cell Rep.* **22**, 3072–3086 (2018).
37. R Development Core Team *R: A Language and Environment for Statistical Computing* (R Foundation for Statistical Computing, 2013).
38. Wickham, H. & Francois, R. dplyr: A grammar of data manipulation. R package version 0.4.**3** (2015).
39. Murrell, P. The grid graphics package. *R. News* **2**, 14–19 (2002).
40. Wickham, H. reshape2: Flexibly reshape data: a reboot of the reshape package. R package version 1 (2012).

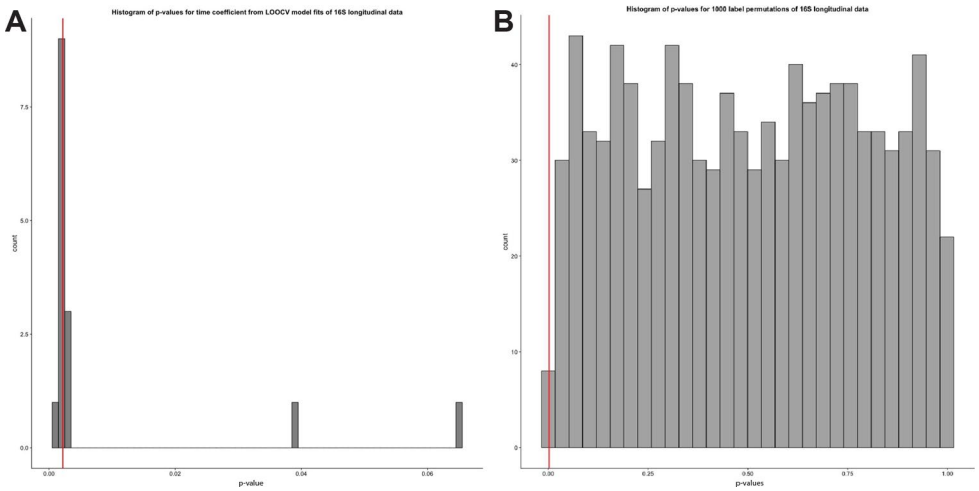

Extended Data Fig. 1 | Statistical validations of association between *Veillonella* abundance and marathon running. a, Histogram of *P* values (Wald Z-tests) for time coefficient from LOOCV models predicting 16S *Veillonella* abundance. The red line represents the *P* value for the model trained without any hold outs. **b**, Histogram of *P* values for time coefficients from 1,000 label permutations in GLMM models predicting *Veillonella* relative abundance. The red line represents the *P* value for the model trained without any label permutation.

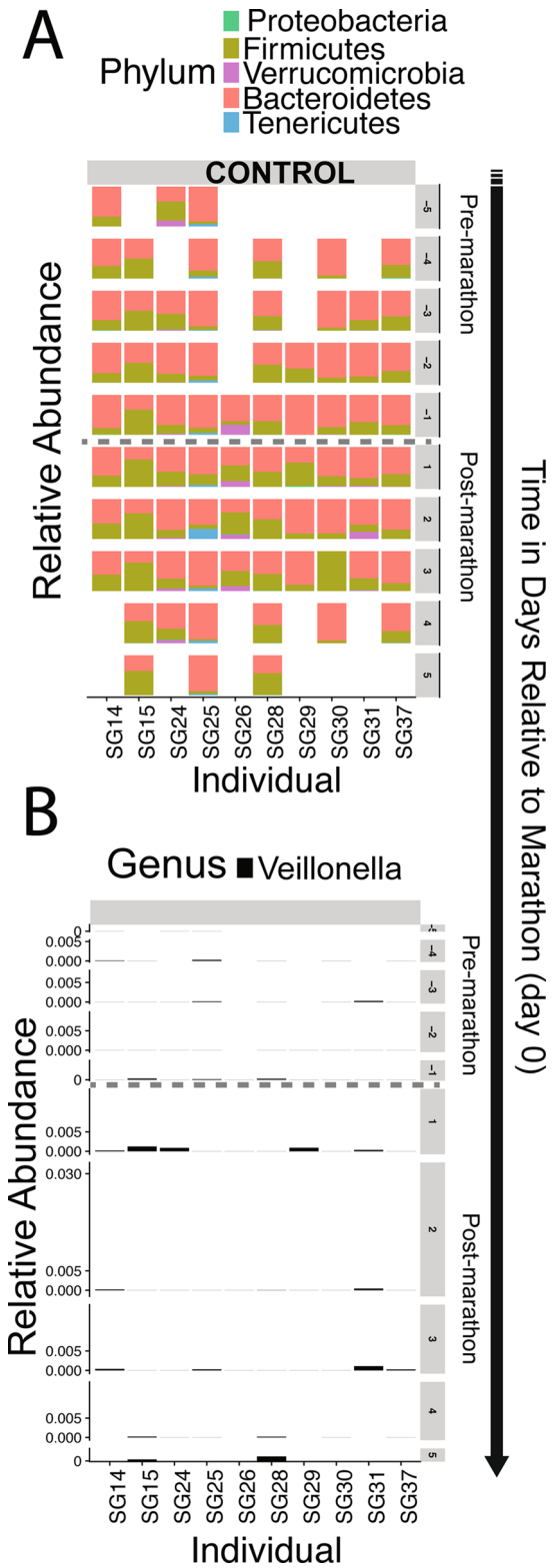

Extended Data Fig. 2 | Microbiome composition in control subjects. a, 16S composition in control subjects. **b**, *Veillonella* relative abundance in control subjects.

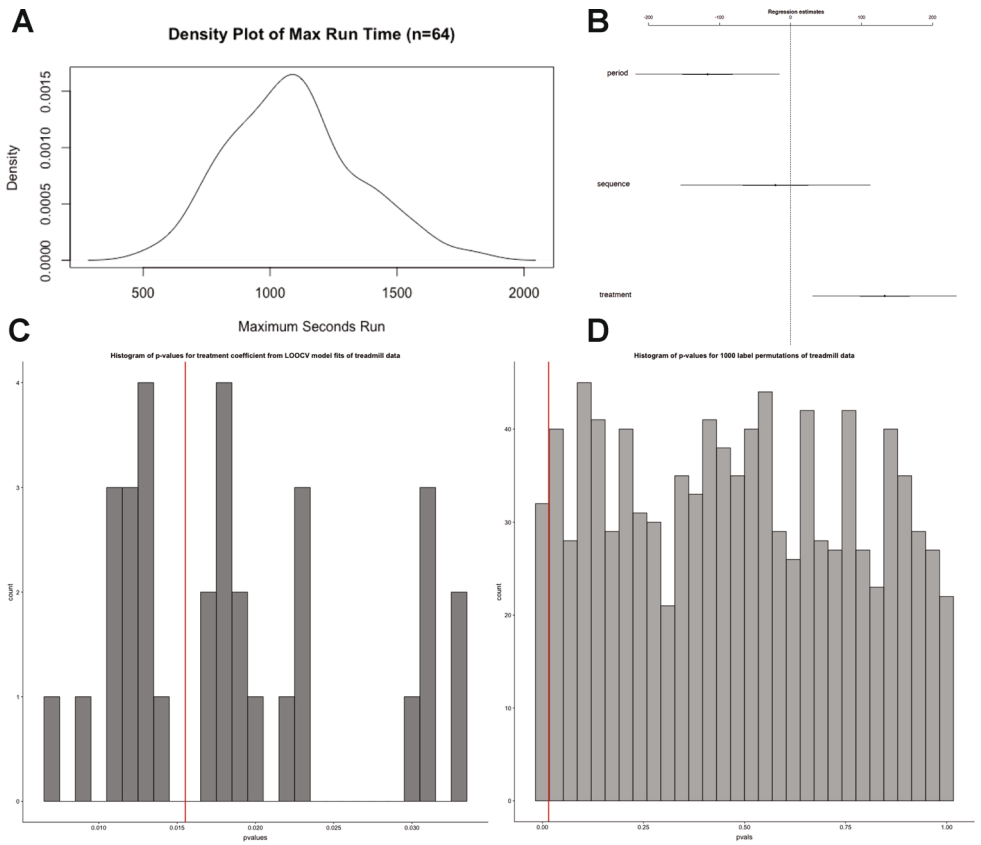

Extended Data Fig. 3 | Statistical validations of the association between *Veillonella* gavage and mouse treadmill run time. a, Density plot of maximum run times in the AB/BA crossover study. A two-sided Shapiro–Wilk normality test on the maximum run times for each mouse in each treatment group resulted in $P = 0.67$, with the null hypothesis that the distribution of data is normal ($n = 64$). **b**, 95% confidence intervals for the coefficient effect on treadmill run time in AB/BA crossover (Wald Z-tests, $n = 64$). Center values are the regression estimate for each coefficient. Error bars represent the 95% confidence interval. **c**, Histogram of *P* values for the treatment coefficient from LOOCV models predicting treadmill run time. The red line represents the *P* value for the model trained without any hold outs (Wald Z-tests, $n = 64$). **d**, Histogram of *P* values for the treatment coefficient from 1,000 label permutations in GLMM models predicting treadmill run time. The red line represents the *P* value for the model trained without any label permutation (Wald Z-tests, $n = 64$ per permutation).

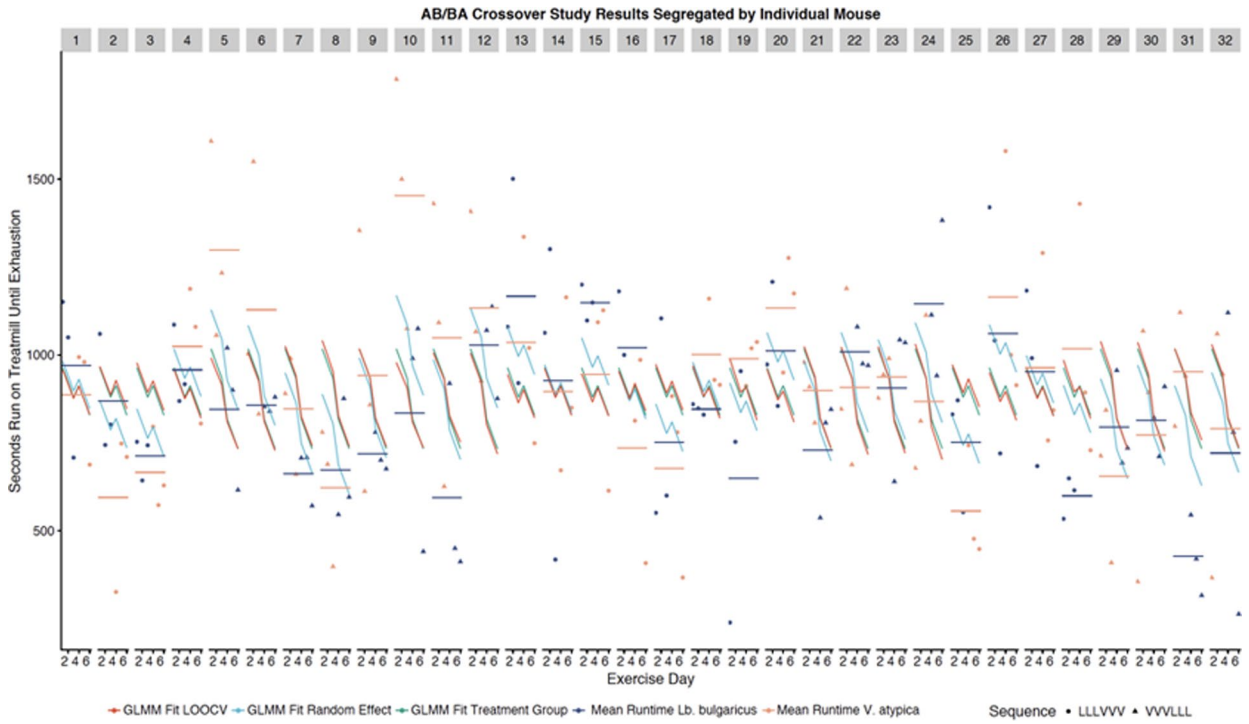

Extended Data Fig. 4 | AB/BA crossover study results segregated by individual mouse. Each of the 32 facets (each representing an individual mouse) has six longitudinal treadmill run times plotted (three pre- and three post-treatment crossover). The shapes of the points represent the treatment sequence. Each mouse facet has two horizontal lines showing the mean run time when dosed with *L. bulgaricus* (light blue) or *V. atypica* (light red). Each facet has a GLMM fit to all data in a treatment sequence (green), a LOOCV GLMM fit trained on all mice except for the mouse the facet represents (red), and a GLMM fit showing the change in intercept related to random effect for each mouse (blue).

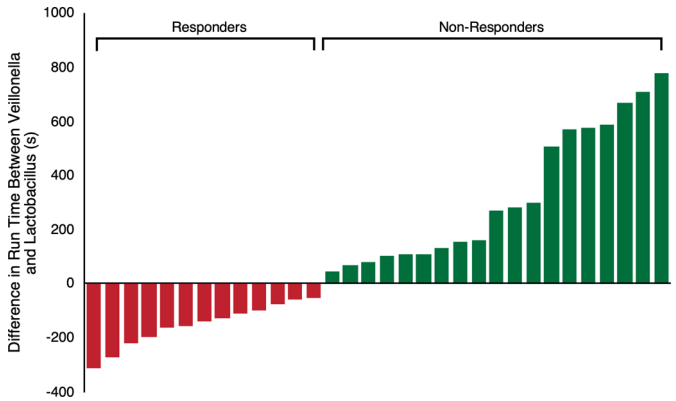

Extended Data Fig. 5 | Difference in maximum treadmill run time. Difference in maximum run time between *V. atypica* and *L. Bulgaricus* gavage treatment periods, segregated into 'responders' and 'non-responders' to *V. atypica* treatment ($n = 32$).

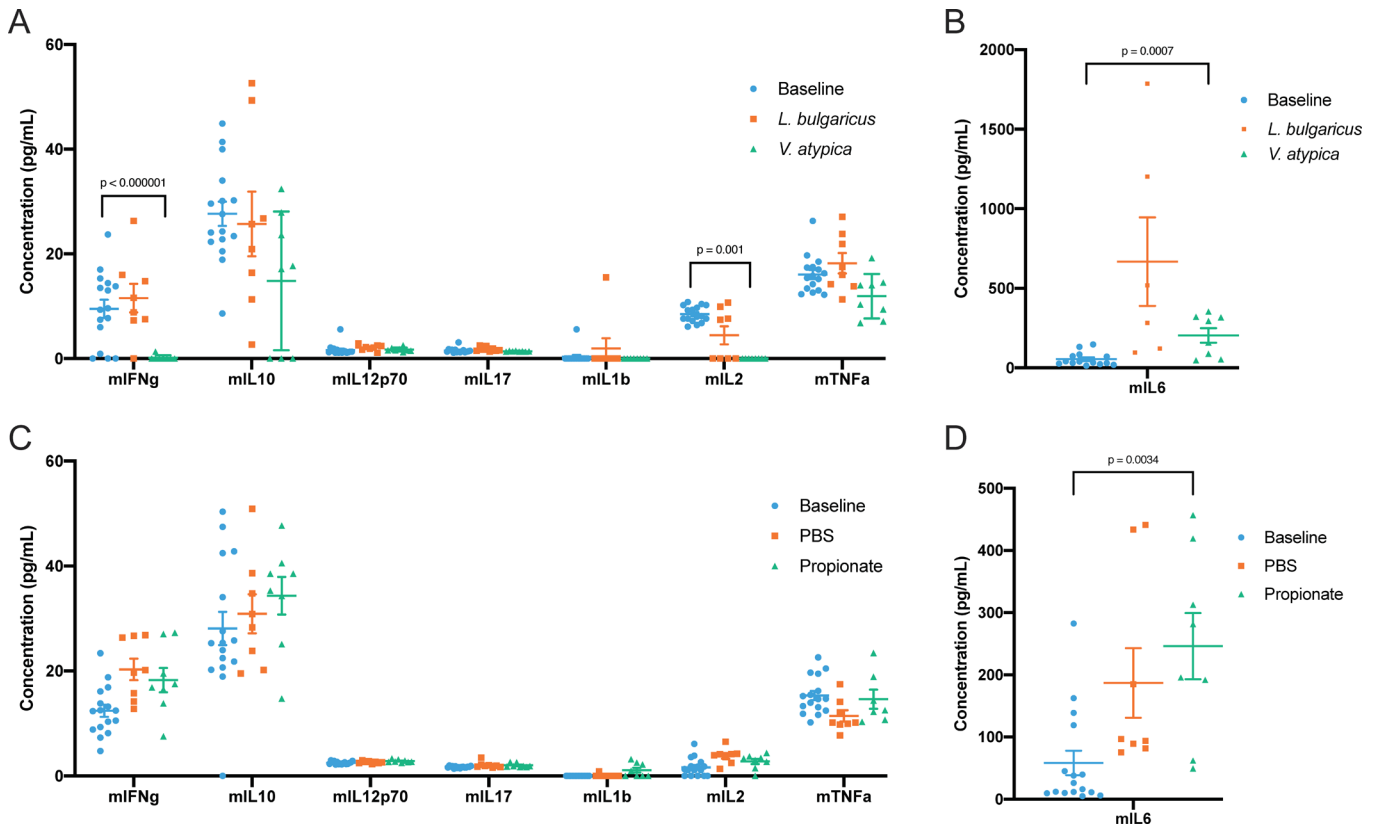

Extended Data Fig. 6 | Mouse serum cytokine response. a,**b**, Cytokines after *V. atypica* and *L. bulgaricus* gavage. Each mouse sample is represented as an individual point, with the central bar representing the mean and error bars representing s.e.m. ($n = 64$, 32 and 32 for baseline, *L. bulgaricus* and *V. atypica*, respectively). **c**,**d**, Cytokines after intrarectal propionate instillation. Each mouse sample is represented as an individual point, with the central bar representing the mean and error bars representing s.e.m. ($n = 32$, 16 and 16 for baseline, *L. bulgaricus* and *V. atypica*, respectively). *P* values were determined by one-way ANOVA followed by Tukey's posthoc test.

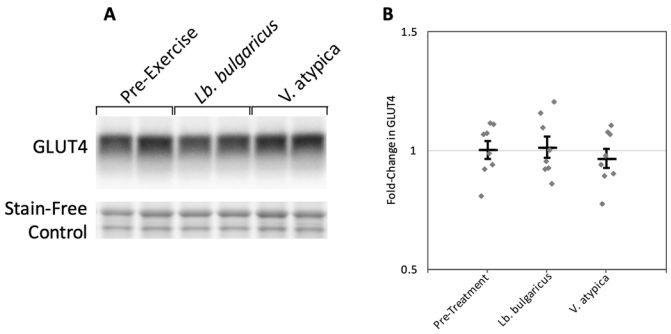

Extended Data Fig. 7 | GLUT4 measurement in mice following gavage. a, Representative section of western blot showing GLUT4 abundance in pre-exercise states, as well as following *L. bulgaricus* and *V. atypica* gavage. A stain-free control was used to normalize the densitometry analysis shown. The experiment was performed once ($n=8$). **b**, Fold-change in GLUT4 abundance. Each point represents an individual mouse sample, the centre bar represents the mean and error bars represent s.e.m. ($n=8$).

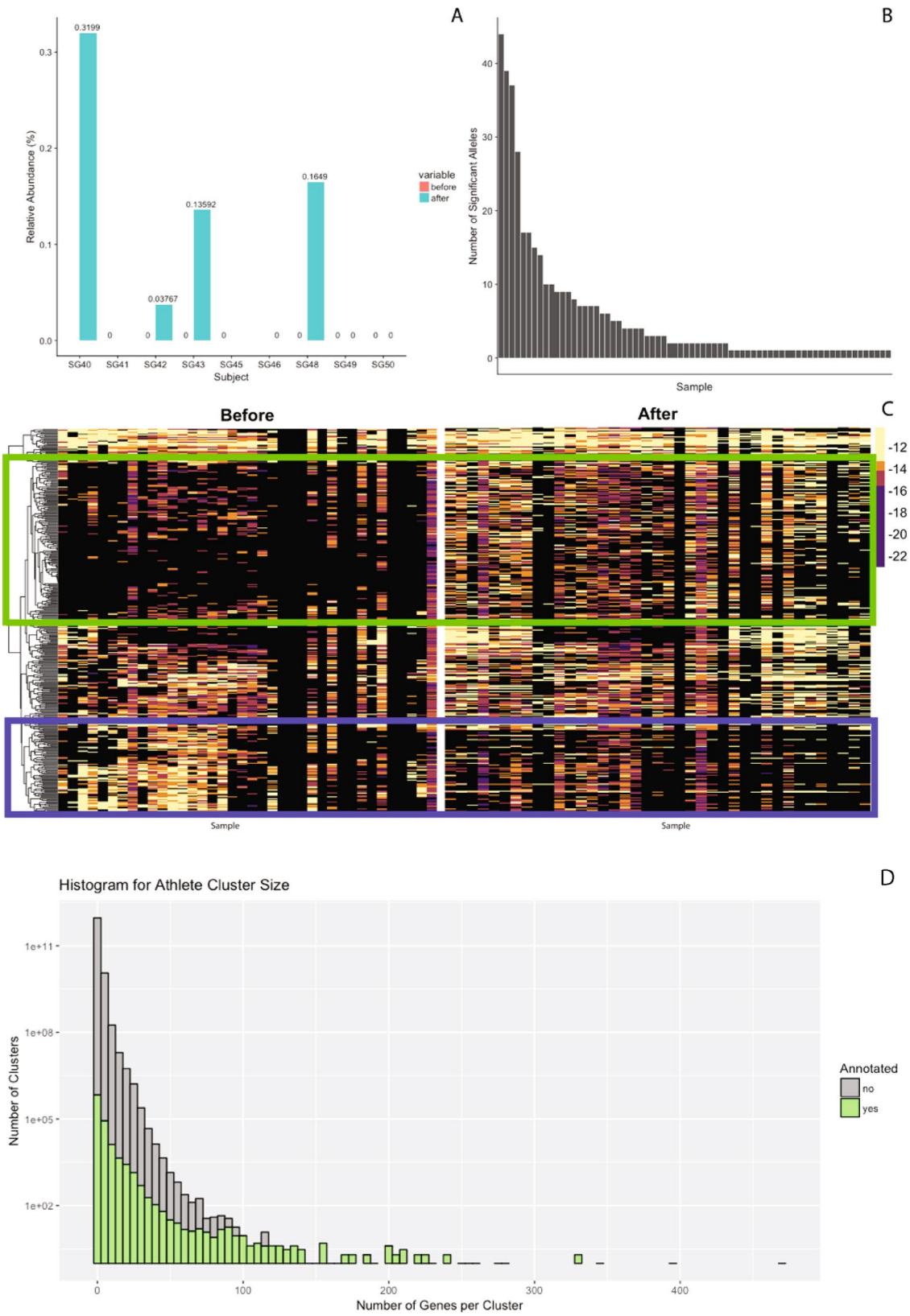

Extended Data Fig. 8 | Metagenomic analysis of athlete gut microbiome samples. a, Fraction of putative *Veillonella* relative abundance from metagenomics (calculated utilizing MetaPhlAn2) before and after exercise in rowers and runners. **b**, Significant alleles (calculated from pairwise ANOVA) that are present in each of the 87 samples. **c**, The aforementioned 396 significant alleles segregated by exercise state and sample. **d**, Histogram comparing non-redundant gene family size and annotation fraction.

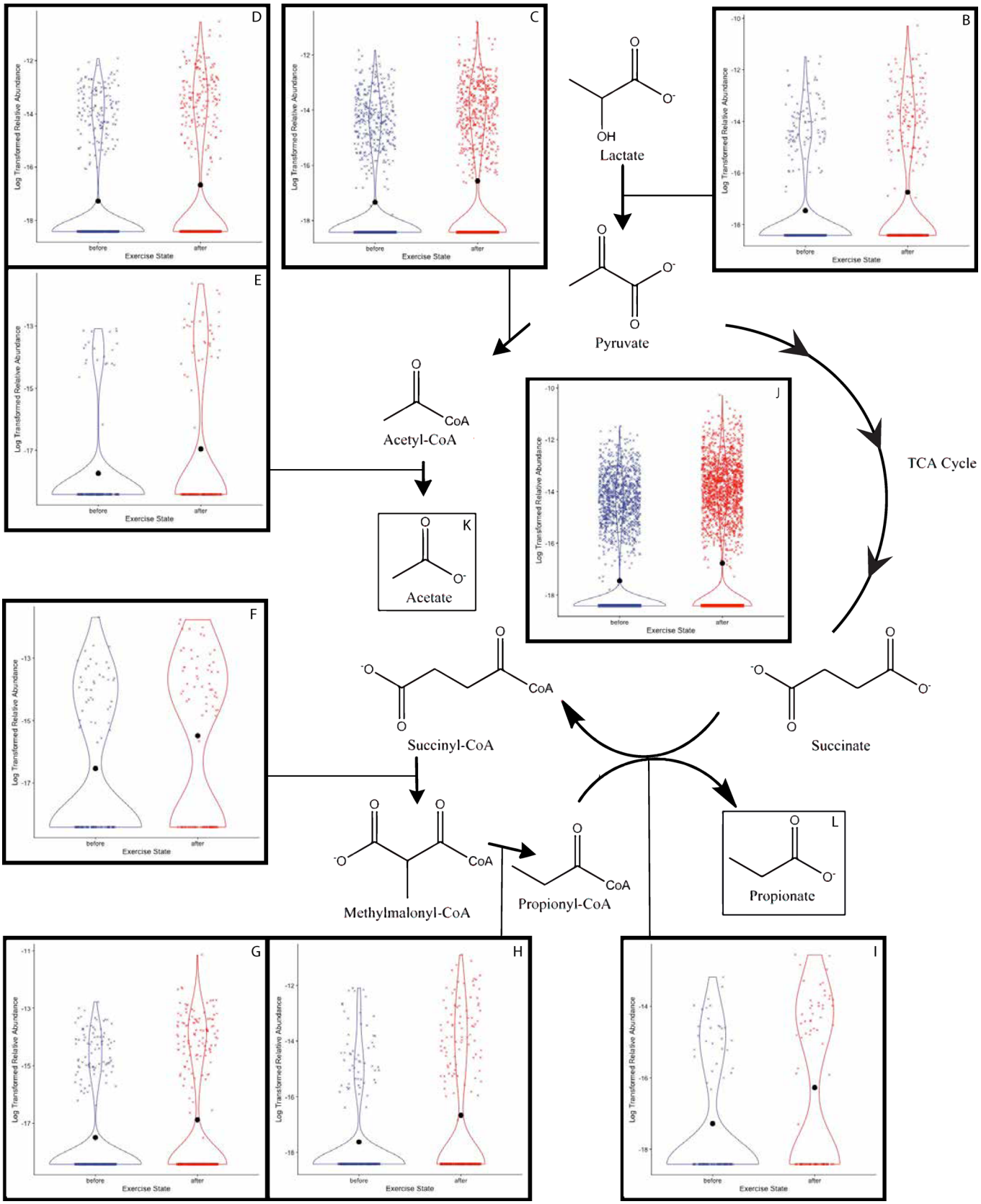

Extended Data Fig. 9 | Enzyme-level abundance analysis of the methylmalonyl-CoA pathway. Enzyme-resolution, log-transformed relative abundances of differentially abundant non-redundant gene families mapped by EC ID to methylmalonyl-CoA pathway components. **a**, Pathway in aggregate. **b**–**i**, Individual reactions in the pathway ($n = 8$). Data are represented as violin plots, which display the distribution of data as a rotated kernel density distribution.

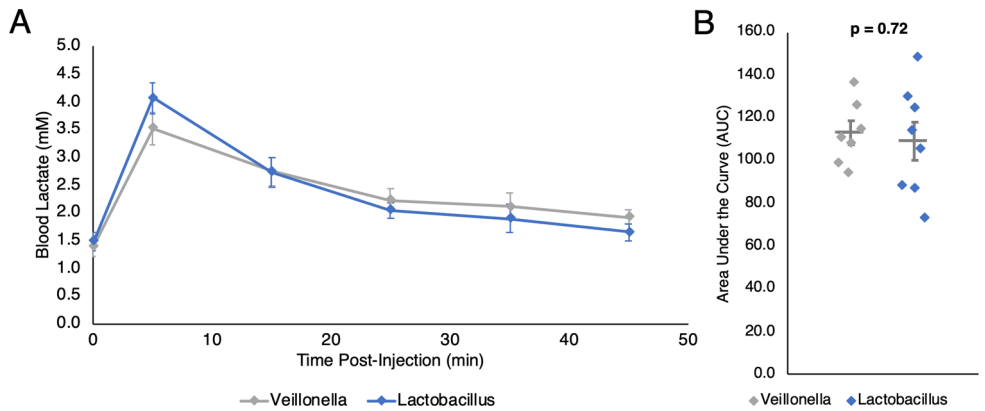

Extended Data Fig. 10 | Lactate clearance following IP injection in mice. a, Mice were gavaged either *V. atypica* or *L. bulgaricus* and, 5 h later, injected with sodium lactate (750 mg kg^{-1}). Blood lactate was measured 5 min postinjection and every subsequent 10 min ($n = 8$). Points are means ± s.e.m. **b**, Area under the curve (AUC) was determined for each mouse and compared between treatments. Each mouse is represented as an individual point, with the central bar representing the mean and error bars representing s.e.m. ($P = 0.72$ by two-sided unpaired t-test, $n = 8$).

nature research

Corresponding author(s): Aleksandar D. Kostic and George M. Church

Last updated by author(s): Apr 25, 2019

Reporting Summary

Nature Research wishes to improve the reproducibility of the work that we publish. This form provides structure for consistency and transparency in reporting. For further information on Nature Research policies, see Authors & Referees and the Editorial Policy Checklist.

Statistics

For all statistical analyses, confirm that the following items are present in the figure legend, table legend, main text, or Methods section.

n/a	Confirmed
☐	☒ The exact sample size (*n*) for each experimental group/condition, given as a discrete number and unit of measurement
☐	☒ A statement on whether measurements were taken from distinct samples or whether the same sample was measured repeatedly
☐	☒ The statistical test(s) used AND whether they are one- or two-sided *Only common tests should be described solely by name; describe more complex techniques in the Methods section.*
☐	☒ A description of all covariates tested
☐	☒ A description of any assumptions or corrections, such as tests of normality and adjustment for multiple comparisons
☐	☒ A full description of the statistical parameters including central tendency (e.g. means) or other basic estimates (e.g. regression coefficient) AND variation (e.g. standard deviation) or associated estimates of uncertainty (e.g. confidence intervals)
☐	☒ For null hypothesis testing, the test statistic (e.g. *F*, *t*, *r*) with confidence intervals, effect sizes, degrees of freedom and *P* value noted *Give P values as exact values whenever suitable.*
☐	☒ For Bayesian analysis, information on the choice of priors and Markov chain Monte Carlo settings
☐	☒ For hierarchical and complex designs, identification of the appropriate level for tests and full reporting of outcomes
☐	☒ Estimates of effect sizes (e.g. Cohen's *d*, Pearson's *r*), indicating how they were calculated

Our web collection on statistics for biologists contains articles on many of the points above.

Software and code

Policy information about availability of computer code

Data collection	no software was used
Data analysis	Unless otherwise noted, all plots were generated in R version 3.4.1 with the ggplot2, dplyr, scales, grid, and reshape2 packages. Large scale data analysis was done on AWS utilizing machines running Ubuntu 16.04. Data curation methods were coded in python version 2.7.12. Unless otherwise noted specifically in the rest of the methods section, code utilized is available to access at https://github.com/kosticlab/athlete and https://github.com/kosticlab/aether. Putative taxonomic abundances were calculated with Metaphlan2. 16S reads were processed with the dada2 pipeline and phyloseq. 16S Veillonella relative abundance modeling for athletes participating in the marathon was done with the R nlme package. Coefficients were were created with the coefplot2 package. Phylogenetic trees were generated from NCBI taxonomy and visualized with phylo.io. All steps in the the processing of raw metagenomic data were done utilizing the Aether package. Raw reads were de novo assembled using megahit. Open reading frames and annotations were generated using prokka. A gene family catalog was generated from the called open reading frames at 95% identity utilizing the CD-HIT software package. A raw abundance count matrix was generated utilizing the gene family catalog, bowtie2, and samtools. The raw abundance count matrix was normalized both by sample and by gene length. Metabolic pathways were queried using MetaCyc and EC IDs were pulled from prokka annotations. Heatmaps were generated with the pheatmap package in R.R was utilized to perform the majority of statistical tests with the exception of pairwise ANOVA tests, for which the SciPy library in python was used. Root mean square error calculations were performed using the plotrix package. The canopy algorithm utilized is available here: https://bitbucket.org/HeyHo/mgs-canopy-algorithm/wiki/Home. Reactions involved with the breakdown of lactate to both propionate and acetate were manually associated with EC IDs using MetaCyc.

For manuscripts utilizing custom algorithms or software that are central to the research but not yet described in published literature, software must be made available to editors/reviewers. We strongly encourage code deposition in a community repository (e.g. GitHub). See the Nature Research guidelines for submitting code & software for further information.

Data

Policy information about availability of data

All manuscripts must include a data availability statement. This statement should provide the following information, where applicable:

- Accession codes, unique identifiers, or web links for publicly available datasets
- A list of figures that have associated raw data
- A description of any restrictions on data availability

All raw sequencing data has been uploaded to NCBI and SRA in the form of the BioProjects PRJNA472785 (16S) and PRJNA472768 (MGX) which are linked to associated BioSamples which are in turn linked to the paired end read files on SRA and correspond to the metadata in the supplement. Additionally, all sequencing files are also available to download from a web browser at https://s3.amazonaws.com/athlete-sequencing-data/index.html.

Field-specific reporting

Please select the one below that is the best fit for your research. If you are not sure, read the appropriate sections before making your selection.

☒ Life sciences ☐ Behavioural & social sciences ☐ Ecological, evolutionary & environmental sciences

For a reference copy of the document with all sections, see nature.com/documents/nr-reporting-summary-flat.pdf

Life sciences study design

All studies must disclose on these points even when the disclosure is negative.

Sample size	No sample size calculation was performed. Leading up to the 2015 Boston Marathon, we attempted to recruit as many participating athletes as possible and collect as many samples as possible from each participant one week before and one week after the race. An equal amount of sedentary controls were then recruited for participation. These sample sizes were sufficient to observe a statistically robust association between Veillonella abundance and time after marathon.
Data exclusions	No data were excluded from the analysis.
Replication	Animal research studies were performed a minimum of three times. All attempts at replication were successful.
Randomization	All animals were randomly allocated into experimental groups.
Blinding	Investigators were blinded to group allocation during data collection and analysis.

Reporting for specific materials, systems and methods

We require information from authors about some types of materials, experimental systems and methods used in many studies. Here, indicate whether each material, system or method listed is relevant to your study. If you are not sure if a list item applies to your research, read the appropriate section before selecting a response.

Materials & experimental systems

n/a	Involved in the study
☒	☐ Antibodies
☒	☐ Eukaryotic cell lines
☒	☐ Palaeontology
☐	☒ Animals and other organisms
☐	☒ Human research participants
☒	☐ Clinical data

Methods

n/a	Involved in the study
☒	☐ ChIP-seq
☒	☐ Flow cytometry
☒	☐ MRI-based neuroimaging

Animals and other organisms

Policy information about studies involving animals; ARRIVE guidelines recommended for reporting animal research

Laboratory animals	All laboratory animals were male Mus musculus strain C57BL/6J aged 8-12 weeks.
Wild animals	The study did not involve wild animals.
Field-collected samples	The study did not involve samples collected from the field.
Ethics oversight	Animal research was approved by the Joslin Diabetes Center IACUC. We have complied with all relevant ethical regulations.

Note that full information on the approval of the study protocol must also be provided in the manuscript.

Human research participants

Policy information about studies involving human research participants

Population characteristics	Athlete 26 total (15 marathon) 65% female (73%) Average age is 27.4 (27.1) Average BMI = 22.4 (22.4) 85% white, 11.5% asian, 4% mixed (73%, 20%, 7%, respectively) 100% from US (96%) Controls 12 total (11 marathon study) 50% female (55%) Average age = 29.5 (29.2) Average BMI = 22.7 (22.9) 50% white, 33% asian, 8% black (45%, 36%, 9% respectively) 58% from US (55%)
Recruitment	Participants were recruited via IRB approved flyers and word of mouth. Our study design relied on prospective selection of the participants, therefore the concern of self-selection bias with regard to outcomes has been eliminated. Each potential participant went though a screening process prior to enrollment to assess study exclusion criteria, which included recent use of antibiotics, pregnancy, travel abroad, or recent inflammatory bowel states. Additionally, participants were determined to be athletes or controls based on screening questions that determined frequency of exercise and training for upcoming athletic competitions.
Ethics oversight	All study participants were recruited following an IRB approved Sports Genomics protocol (#IRB15-0869), conducted at the Wyss Institute for Biologically Inspired Engineering. Each participant read and signed a consent form prior to study enrollment. We have complied with all relevant ethical regulations.

Note that full information on the approval of the study protocol must also be provided in the manuscript.